POLITECNICO DI TORINO
Repository ISTITUZIONALE

Microplastic fiber release from woven synthetic fabrics during washing: structural and mechanical drivers of shedding

Original
Microplastic fiber release from woven synthetic fabrics during washing: structural and mechanical drivers of shedding / Akyildiz, S.H., Pereira, M., Bellopede, R., López-Beceiro and Ramón Artiaga, J.. - In: FRONTIERS IN MATERIALS. - ISSN 2296-8016. - 13:(2026). [10.3389/fmats.2026.1891868]

Availability:
This version is available at: 11583/3018448 since: 2026-11-26T07:59:23Z

Publisher:
Frontiers Media

Published
DOI:10.3389/fmats.2026.1891868

Terms of use:

This article is made available under terms and conditions as specified in the corresponding bibliographic description in the repository

Publisher copyright

(Article begins on next page)

29 November 2026

frontiers in Materials

TYPE Original Research
PUBLISHED 19 November 2026
DOI 10.3389/fmats.2026.1891868

Check for updates

OPEN ACCESS

EDITED BY
Francesca De Falco,
University of Bayreuth, Germany

REVIEWED BY
Lin Feng Ng,
University of Technology Malaysia, Malaysia
Vasiliki Soursou,
University of Valencia, Spain

*CORRESPONDENCE
Sinem Hazal Akyıldız,
sinem.akyildiz@polito.it
Mercedes Pereira,
mercedes.pereira@udc.es

RECEIVED 26 May 2026
REVISED 16 September 2026
ACCEPTED 28 September 2026
PUBLISHED 19 November 2026

CITATION
Akyıldız SH, Pereira M, Bellopede R, López-Beceiro J and Artiaga R (2026) Microplastic fiber release from woven synthetic fabrics during washing: structural and mechanical drivers of shedding.
Front. Mater. 13:1891868.
doi: 10.3389/fmats.2026.1891868

COPYRIGHT
© 2026 Akyıldız, Pereira, Bellopede, López-Beceiro and Artiaga. This is an open-access article distributed under the terms of the Creative Commons Attribution License (CC BY). The use, distribution or reproduction in other forums is permitted, provided the original author(s) and the copyright owner(s) are credited and that the original publication in this journal is cited, in accordance with accepted academic practice. No use, distribution or reproduction is permitted which does not comply with these terms.

Microplastic fiber release from woven synthetic fabrics during washing: structural and mechanical drivers of shedding

Sinem Hazal Akyıldız[1]*, Mercedes Pereira[2]*, Rossana Bellopede[1], Jorge López-Beceiro[2] and Ramón Artiaga[2]

[1]Department of Environment, Land and Infrastructure Engineering, Politecnico di Torino, Torino, Italy, [2]Centro de Investigacións en Tecnoloxías Navais e Industriais, Universidade da Coruña, Ferrol, Spain

Laundering synthetic textiles is a major pathway for microplastic fiber (MPF) release, yet the fabric-level structural and mechanical factors controlling shedding remain insufficiently understood. This study investigated MPF release from eight woven continuous-filament synthetic fabrics, including virgin polyester (PET), recycled polyester (rPET), polyamide (PA), PA/PET, and PA/elastane fabrics with plain, twill, and satin constructions. Standardized washing tests were performed according to ISO 4484–1:2023, and MPF release was assessed using mass-based, count-based, and fiber-length metrics. Among the tested fabrics, PET2 and rPET exhibited the highest normalized MPF release, at 31.67 and 30.74 MPFs/g, respectively, whereas PET3 and PET4 showed the lowest release, at 9.51 and 8.48 MPFs/g. These results suggest that fabric openness, yarn density, weave structure, and fiber origin may influence MPF shedding. Notably, rPET released approximately 2.3-fold more MPFs/g than structurally comparable PET1, indicating that recycled polyester may behave differently during laundering even when fabric construction is similar. Fiber-length distributions further indicated differences in fragmentation behavior, with rPET, PET3, and PET4 producing greater proportions of short fibers (<0.5 mm). Exploratory PCA, with the first two components explaining 65.1% of the total variance, suggested that MPF release was associated with yarn density, fabric compactness, binding coefficient, and mechanical response rather than polymer composition alone. These findings demonstrate that MPF shedding from woven synthetic fabrics is governed by multiscale interactions between fabric structure and mechanical behavior and highlight opportunities to reduce MPF release through textile design.

KEYWORDS
laundering emissions, microplastic fiber release, pollution, polyester textiles, shedding behavior, textile microplastics

1 Introduction

Microplastics have emerged as one of the most pervasive anthropogenic pollutants of the 21st century, raising growing environmental and public health concerns due to their persistence, bioaccumulation potential, and ubiquity in terrestrial and aquatic ecosystems. Among microplastic morphologies, fibrous particles—commonly termed microfibers—are now recognized as one of the dominant forms detected in wastewater, sludge, sediments,

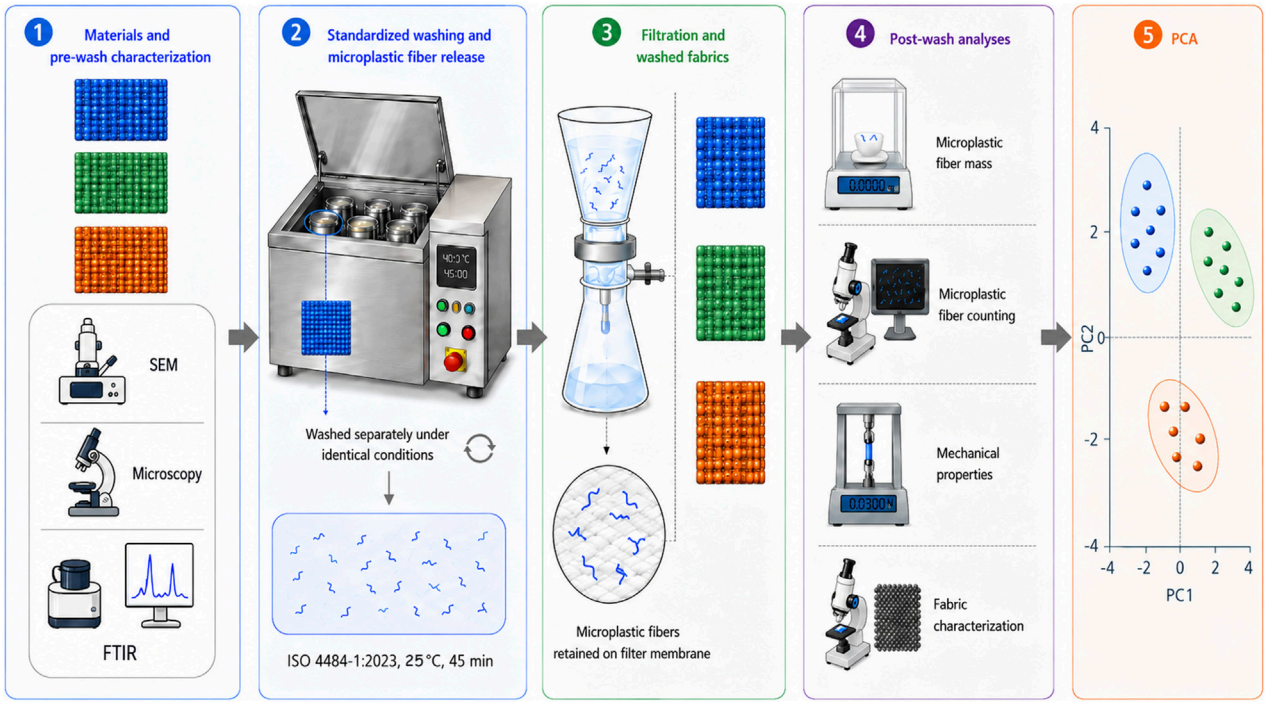

GRAPHICAL ABSTRACT

and biota (Liu et al., 2019; Suaria et al., 2020; Balestra et al., 2024; Akyıldız et al., 2025). In environmental research, the term microfiber refers to fibrous particles < 5 mm regardless of composition, whereas synthetic fibrous particles are defined as microplastic fibers (Akyıldız et al., 2025; Henry et al., 2019). Among the various sources of microplastic contamination, synthetic textiles represent a major contributor, primarily through the release of MPFs during manufacturing, use, and laundering processes (Napper and Thompson, 2016; De Falco et al., 2019; Balasaraswathi and Rathinamoorthy, 2022; Ghosh et al., 2023). Global fiber production continues to increase, rising from 125 million tons in 2023 to 132 million tons in 2024, with projections reaching 169 million tons by 2030 (Textile Exchange, 2025). Synthetic fibers account for approximately 69% of total fiber production, and polyester alone represents nearly 60% (Textile Exchange, 2025). This dominance of synthetic materials directly contributes to the increasing environmental load of textile-derived microplastics. MPFs pose environmental risks due to their persistence and potential to transport or release hazardous substances. Unlike natural fibers, synthetics such as polyester and polyamide can persist in the environment for years, especially in sediments and soils where degradation is minimal (Das et al., 2024; Priyadarshini et al., 2024; Dey et al., 2024). Polyester and polyamide have also been reported among the most frequently detected fibrous polymers in sludge (Gambino et al., 2025). Additionally, these fibers often carry hazardous additives—including dyes, softeners, and flame retardants—that may leach into water and accumulate in organisms (Periyasamy, 2023; Chakraborty et al., 2024; Sharma et al., 2024). Moreover, microplastic fibers can adsorb co-existing contaminants such as pesticides and heavy metals, acting as vectors that enhance trophic transfer and ecological risk (Kumar et al., 2024; Paul et al., 2024). This persistence and pollutant-loading capacity raise concerns not only for ecosystem health but also for potential human exposure through contaminated water, food, air, and indoor environments (Das et al., 2024; Chakraborty et al., 2024). Human exposure to microplastics is increasingly recognized to occur through ingestion, inhalation, and possibly dermal contact (Nawab et al., 2024). For microplastic fibers, inhalation and indoor exposure are particularly relevant because synthetic textiles, carpets, upholstery, furniture, and household dust can contribute fibrous particles to indoor environments (Dris et al., 2017; Noorimotlagh et al., 2024). Recent reviews on airborne microplastics and lung exposure indicate that inhaled microplastics may deposit in the respiratory tract depending on their size, shape, and aerodynamic behavior, with potential implications for oxidative stress, inflammation, impaired lung function, and respiratory health (Gou et al., 2024; Saha and Saha, 2024; Vattanasit et al., 2023). However, major uncertainties remain regarding exposure dose, retention, clearance, translocation, and long-term effects, especially for MPFs (Gou et al., 2024; Vattanasit et al., 2023). Therefore, studies that identify textile parameters controlling MPF release can contribute indirectly to human-health protection by supporting source-level mitigation strategies.

Most studies on microfiber release have focused on external laundering conditions, such as temperature, detergents, and washing devices, while intrinsic textile parameters have received comparatively less attention (De Falco et al., 2018; Cai et al., 2020; Periyasamy and Tehrani-Bagha, 2022; Sheikhi et al., 2024).

However, increasing evidence indicates that fabric structure and fiber morphology play a critical role in influencing fiber detachment. Parameters such as weave type, yarn configuration, interlacing density, yarn compactness, and mechanical response influence fiber mobility, inter-fiber cohesion, and resistance to mechanical stress during washing (Raja Balasaraswathi and Rathinamoorthy, 2021; Han et al., 2024). These structural factors are therefore essential to understanding shedding mechanisms. Moreover, fiber type and origin significantly influence shedding behavior. Acrylic and polyamide fabrics have been reported to release longer or more numerous MPFs in some studies, partly due to differences in elongation, tensile behavior, and abrasion resistance (Vassilenko et al., 2021; Frost et al., 2020; Nyssanbek et al., 2022). Cesa et al. (2020) further demonstrated that, among polyamide, acrylic, and polyester fabrics, acrylic released the highest amount of MPFs, followed by polyamide, while polyester exhibited the lowest shedding tendency. However, even within polyester, the source of the fiber—whether virgin or recycled—adds complexity to the issue. The impact of recycling on MPF shedding is still under debate. Some studies suggest that recycled polyester (rPET) sheds more due to structural degradation during the recycling process, including reduced molecular weight and altered crystallinity, which may compromise mechanical integrity (Özkan and Gündoğdu, 2020; Akyildiz et al., 2024). Others, however, report no significant difference in shedding between virgin and recycled polyester, suggesting that fabric structure and surface treatments may have a greater influence than fiber origin alone (Frost et al., 2020; Gao et al., 2024). Recent studies on fibrous polymer systems further support this perspective by showing that recycling pathways, processing history, fiber morphology, and structural characterization can influence the performance and sustainability of polymer-based fibrous materials (Das et al., 2026; Das and Jesionek, 2024). Therefore, fiber origin should be considered together with fabric-level structural and mechanical properties when evaluating MPF release from virgin and recycled polyester fabrics. Despite recent progress, the relative contribution of fiber-level morphology, yarn compactness, weave structure, and mechanical response to MPF release remains insufficiently understood, particularly for woven continuous-filament synthetic fabrics. In addition, the absence of standardized testing methods has limited the comparability of previous studies. The introduction of ISO 4484-1 (2023) provides a controlled framework for reproducible assessment of microfiber release during laundering. Standardized testing is particularly important because particle number, length distribution, and mass-based indicators may provide complementary information on MPF release and potential exposure relevance.

The novelty of this study lies in its integrated evaluation of woven fabric construction, yarn-level structural parameters, and mechanical behavior as combined drivers of MPF release under a standardized washing protocol. By combining standardized laundering experiments with multiscale material characterization and principal component analysis (PCA), this work identifies key structural and mechanical parameters associated with microfiber detachment from continuous-filament woven synthetic fabrics.

2 Materials and methods

2.1 Materials

Eight woven synthetic fabrics were selected, differing in fiber composition and structural characteristics. The materials included four virgin polyester (PET) fabrics, one recycled polyester (rPET), one polyamide (PA), and one polyamide/polyester blend coded as PAPET, and one polyamide/elastane blend coded as PAEL. Six fabrics had a plain weave structure, while two PET fabrics were constructed with twill (PET3) and satin (PET4) weaves. The fabric samples used in this study were obtained from commercial and industrial textile sources, including Zeus Textile Company, Inditex, and Technical Advice companies. Detailed information on composition, blend ratios, and fabric structure is provided in Table 1. Additional fiber-, yarn-, and fabric-level parameters are reported in Supplementary Table S1, including yarn linear density, fabric areal density, thickness, yarn density, fiber diameter, and binding coefficient. The binding coefficient describes the degree of yarn interlacing within the fabric; a value of 1 corresponds to plain weave structures, which have the highest interlacing density among the fabrics examined.

The fabric set was selected to cover a range of structural and compositional characteristics relevant to woven synthetic textiles commonly used in apparel and fast-fashion products. The selected fabrics differed in polymer composition, fiber origin, weave structure, yarn density, filament morphology, and mechanical behavior. PET1 and rPET were included as structurally comparable plain-weave polyester fabrics to examine the influence of recycled fiber origin and mechanical response. PET2 represented a lower-density plain-weave polyester structure, whereas PET3 and PET4 were selected to evaluate twill and satin constructions. PA, PAPET, and PAEL were included to assess the influence of polyamide, PA/PET blending, and elastane-containing structures. Although this fabric set does not represent all commercially available synthetic textiles, it provides a controlled basis for comparing key fabric-level parameters affecting MPF release.

2.2 Methods

The experimental workflow consisted of (i) multiscale material characterization, (ii) standardized laundering experiments, and (iii) statistical data analysis. Fabric properties were characterized at fiber, yarn, and fabric levels using microscopy, spectroscopy, and mechanical testing. Washing experiments were performed in accordance with ISO 4484-1 (2023), which specifies the standardized method for evaluating fiber loss from fabrics during domestic laundering. All samples were subjected to the same controlled conditions without detergent to isolate the influence of fabric-related parameters from detergent-related effects. After each washing test, the effluent was filtered, and the retained MPFs were analyzed by mass- and count-based methods. Following laundering, all fabric specimens were further examined through mechanical testing and post-wash SEM imaging to assess surface degradation and yarn damage. The resulting dataset was analyzed via PCA to identify correlations between textile parameters and MPF release behavior.

10.3389/fmats.2026.1891868

TABLE 1 Composition, structure, and microscopic photos of fabric samples.

Sample code	Fabric color	Composition	(%)	Structure	Microscope photos
PA	White	Polyamide	100	Plain	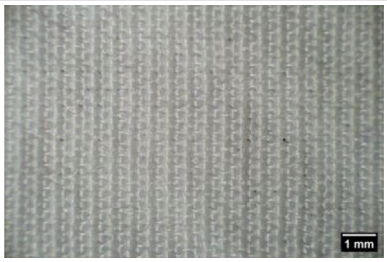
PAEL	Petrol	Polyamide/Elastane	86/14	Plain	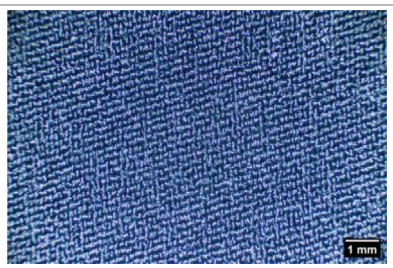
PAPET	Black	Polyamide /PET	50/50	Plain	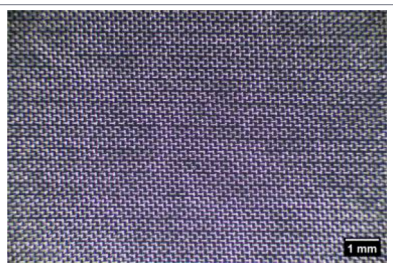
PET1	Light blue	PET	100	Plain	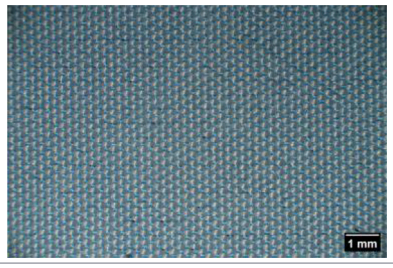
PET2	White	PET	100	Plain	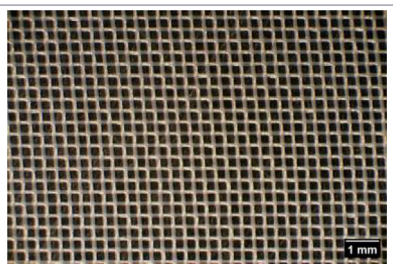
PET3	Green	PET	100	Twill	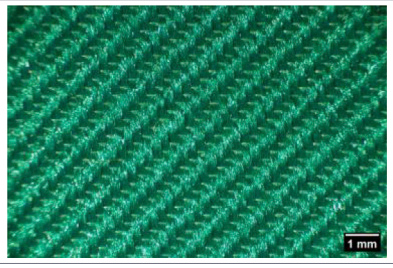

(*Continued*)

TABLE 1 Continued

Sample code	Fabric color	Composition	(%)	Structure	Microscope photos
PET4	Blue	PET	100	Satin	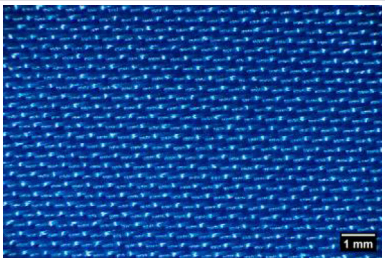
RPET	Brown	rPET	100	Plain	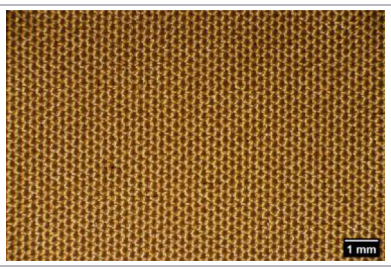

2.3 Characterization of materials

2.3.1 Thermal and mechanical analysis

Dynamic mechanical analysis (DMA) was performed using a Rheometrics DMTA-IV instrument in tensile mode. Rectangular fabric specimens were tested in both warp and weft directions. Frequency sweep tests were conducted from 0.1 to 100 Hz at room temperature, following a preliminary strain sweep to ensure deformation within the linear viscoelastic region (0.01%). Strain ramp tests were performed at a rate of 0.1% s^{-1} with an initial force of 0.05 N. DMA measurements were conducted in triplicate for each fabric type and testing direction. The use of triplicate measurements allowed experimental variability to be assessed and provided representative fabric-level mean values for subsequent comparison.

Thermogravimetric analysis (TGA) was carried out using a simultaneous DSC-TG instrument (TA Instruments). Samples (~10 mg) were heated from room temperature to 700 °C at 10 °C min^{-1} under air atmosphere. Derivative thermogravimetric (DTG) curves were analyzed using Fityk software to identify decomposition steps and estimate compositions in blended fabrics. The method for textile fiber identification in blends has been developed in a previous work, in which the procedure is explained in detail (Pereira et al., 2024). DSC measurements used to compare PET1 and rPET were obtained from the simultaneous DSC-TG instrument under the same heating program, unless otherwise stated. TGA/DTG analyses were conducted in triplicate for each fabric sample. DSC curves obtained from the simultaneous DSC-TG measurements were used for PET1 and rPET comparison. DMA was used to assess mechanical response, whereas TGA/DTG and DSC were used to evaluate thermal degradation behavior and thermal transitions. These properties were then considered in relation to MPF detachment during laundering.

2.3.2 SEM and FTIR

Fourier-transform infrared spectroscopy in attenuated total reflectance mode (ATR-FTIR, Shimadzu AIM-9000) was used to verify chemical composition. SEM imaging (FEI Inspect S) was employed to observe fiber morphology, cross-sectional shape, and yarn structure. Post-wash SEM images provided visual evidence of surface fibrillation, cracking, and fiber-end protrusion, indicating structural degradation and MPF release mechanisms. SEM observations were used qualitatively to support the interpretation of shedding mechanisms rather than as a quantitative measure of MPF release.

2.4 Specimen preparation and washing procedure

According to ISO 4484-1 (2023), fabric specimens were cut to final dimensions of (100 ± 10) mm × (240 ± 10) mm. Edges were thermally sealed by brief flame exposure to prevent fraying. Samples were oven-dried at 50 °C overnight for moisture equilibration before weighing and testing.

The washing tests were conducted in accordance with ISO 4484-1 (2023), which specifies the standardized procedure for assessing fiber loss from fabrics during domestic laundering. Each chamber (200 ± 5 mm diameter, 140 ± 10 mm height) contained 80 stainless steel balls, 1.2 L of Milli-Q water (25 °C), and one fabric specimen. Tests were carried out for 45 min at 100 ± 2 rpm without detergent. Three replicates were performed for each fabric type.

2.5 Cleaning and contamination controls

To minimize contamination, all procedures were carried out using glass and stainless-steel equipment, handled with nitrile gloves, and protected with aluminum foil covers. Prior to the

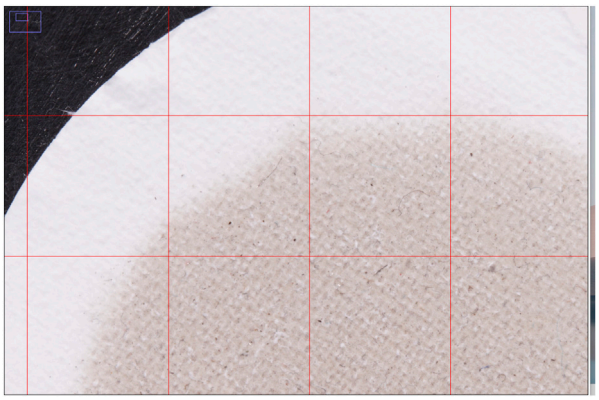

FIGURE 1
Quantification of MPFs on glass fiber filters using macroscopic images with grid overlays, analyzed via ImageJ software.

washing series, all equipment was rinsed with a 1:9 ethanol–water solution and thoroughly cleaned between tests.

To verify cleanliness, blank washes were performed under identical laundering conditions without fabric specimens. These controls confirmed negligible background contamination in the system.

2.6 Filtration, visualization, and counting of MPFs from wash water

The collected effluents were filtered under vacuum using glass fiber filters (Whatman, Ø 47 mm) with a 0.7 μm pore size. Following filtration, the filters were dried at 50 °C for 24 h to remove moisture prior to analysis. After drying, MPFs retained on the filters were weighed, visually identified, counted, and measured their length. Image analysis was carried out using ImageJ software (Figure 1), based on macroscopic images captured under standard lighting conditions using a high-resolution digital single-lens reflex (SLR) camera (Sony ILCE-7RM3 v1.01).

2.7 Data analysis

MPF release was quantified using two gravimetric indicators: fabric mass loss after washing and filter mass gain after effluent filtration. All materials were pre-conditioned at 50 °C for 4 h before testing to ensure consistency. Filter mass was determined using an analytical balance (Sartorius, PRACTUM124-1S) with a precision of 0.1 mg, and filters from contamination controls were excluded from analysis.

MPF shedding was expressed as filter mass gain per fabric mass (mg/g) and MPF count per fabric mass (MPFs/g). ImageJ was used to quantify MPF counts and length distributions from filter images. To evaluate statistical variability, data from eight fabric types (tested in triplicate) were analyzed using one-way ANOVA. Mean values and standard deviations were calculated from triplicate washing experiments for each fabric type. Where applicable, statistical differences among fabrics were evaluated at $p < 0.05$.

PCA was performed in MATLAB using individual replicate data from eight fabric types tested in triplicate, resulting in 24 observations in the PCA input matrix. This approach allowed both between-fabric differences and within-fabric experimental variability to be represented in multivariate analysis. Because the observations were grouped within eight fabric types, PCA was interpreted as an exploratory tool to identify associations among structural, mechanical, and MPF-release variables rather than as a predictive or causal model.

3 Results and discussion

3.1 Characterization of fabrics

3.1.1 Structural characterization

The fabrics were characterized in terms of weave structure, yarn configuration, and fiber-level morphology. The corresponding dimensional parameters, including binding coefficient, basis weight, thickness, yarn density, and fiber diameter, are summarized in Supplementary Table S1. These parameters are expected to influence inter-fiber cohesion, frictional resistance, and stress distribution under mechanical agitation during laundering. Six fabrics exhibited plain weave structures (binding coefficient = 1), corresponding to the highest interlacing density. In contrast, PET3 (twill, 0.5) and PET4 (satin, 0.4) showed lower binding coefficients and longer float lengths. Although reduced interlacing is generally associated with increased fiber mobility, the results suggest that shedding behavior is not controlled by interlacing density alone, but rather by the combined effects of yarn compactness, fabric density, filament morphology, and mechanical response. At the yarn level, variations in yarn density (ends and picks per cm) and yarn count were observed among fabrics. For example, PET2 exhibited lower yarn density than more compact fabrics such as PET3, which may reduce inter-yarn constraint and increase yarn exposure to mechanical agitation, thereby facilitating filament displacement under cyclic washing stress. All fabrics were composed of continuous filaments with varying cross-sectional shapes (circular, oval, and square) and diameters ranging from approximately 10–18 μm. Thinner filaments may be more susceptible to bending fatigue and fibrillation, whereas thicker filaments may detach less frequently but contribute greater mass per released MPF.

3.1.2 FTIR identification

ATR-FTIR spectra were examined to identify the characteristic functional groups of the different fabric compositions. The PA fabric showed typical polyamide absorption bands, including N–H stretching at 3,293 cm^{-1}, amide I/C=O stretching at 1,631 cm^{-1}, amide II bands at 1,536–1,460 cm^{-1}, and C–N stretching at 1,373 cm^{-1}, consistent with reported FTIR-based identification of polyamide fibers (Akyildiz et al., 2023). PET-based fabrics showed characteristic polyester bands, including ester C=O stretching at 1710 cm^{-1}, aromatic ring vibrations at 1,504–1,405 cm^{-1}, ester C–O stretching at 1,242 cm^{-1}, O–C–O/C–O–C stretching at 1,092 cm^{-1}, and aromatic C–H bending at 719 cm^{-1} (Akyildiz et al., 2023).

Therefore, the N–H stretching band was mainly associated with PA-containing samples, including PA, PAPET, and PAEL, whereas the ester C=O stretching band at 1710 cm^{-1} corresponded to PET-based samples, including PET1–PET4, rPET, and the PET component of PAPET. PAPET exhibited bands from both PET and PA, consistent with its blended PA/PET composition. PAEL showed dominant PA-related bands, with weak absorption near 1720 cm^{-1} that may be attributed to urethane carbonyl groups from elastane. No major functional-group differences were observed between PET and rPET, although slight spectral broadening and intensity changes in rPET may indicate microstructural differences associated with recycling. Overall, the ATR-FTIR results were consistent with the assigned fiber compositions, while detailed peak assignments are provided in Supplementary Figure S1.

3.1.3 Mechanical analysis

The stress–strain curves of the tested fabrics are shown in Supplementary Figure S2. Polyester fabrics generally exhibited three deformation regions: an initial low-slope region associated with yarn alignment and crimp extension, a steeper region corresponding to elastic deformation, and a final low-slope region as structural limits were approached. In contrast, the PA fabric showed a more continuous deformation profile, particularly in the warp direction. PAPET displayed an intermediate response between PET and PA fabrics. PAEL showed the most distinct behavior, as the combination of polyamide and elastane allowed high deformation at very low stress, reaching approximately 20% strain in the warp direction and 30% in the weft direction. Direction-dependent differences were also observed. Even in fabrics with the same warp and weft yarn composition, such as rPET, PET1, and PAEL, the warp direction generally showed higher resistance to deformation. Since TGA confirmed that the warp and weft yarns of PAPET had the same composition, the directional differences observed in DMA are more likely related to yarn arrangement and fabric structure than to chemical composition.

Figure 2 shows the average Young's modulus values measured from strain ramp tests in the warp and weft directions. In some fabrics, the warp and weft values were comparable, whereas in others clear direction-dependent differences were observed. The large difference in PET3 arises from the fact that it presents a monofilament weft yarn versus a multifilament warp yarn. The polyamide fabric presents a lower modulus compared to polyester fabrics. This reduction in rigidity was further enhanced by the addition of elastane to PA fibers, as observed for PAEL. In PAPET, the PA/PET blend also showed clear differences between the warp and weft directions, indicating that yarn arrangement and fabric architecture strongly influenced the mechanical response (Figure 2).

It is also worth mentioning the case of PET1 and rPET, which presented the same plain-weave structure: PET1 was more easily deformed than rPET, indicating that rPET exhibited a stiffer mechanical response despite having a similar structure. To further examine the differences between PET1 and rPET, DSC analysis was performed on both fabrics. The heating and cooling curves are shown in Figure 3.

PET1 and rPET exhibited broadly similar melting and crystallization profiles, indicating that no major differences in thermal transition behavior were detected under the conditions used in this study. Therefore, the higher rigidity of rPET observed in DMA cannot be attributed solely to differences in melting or crystallization behavior. Instead, it may arise from other factors not directly resolved by DSC, such as filament spinning history, yarn packing, residual defects, surface damage, or differences in filament-level orientation. These results suggest that the mechanical and shedding behavior of rPET should be interpreted in relation to its measured stiffness and fabric-level structure rather than crystallinity alone. To better approximate the mechanical response of fabrics under cyclic washing conditions, the samples were also tested in dynamic mode. The curves obtained from this analysis are shown in Supplementary Figure S3. Figure 4 presents the average storage modulus values measured during frequency sweep tests in the warp and weft directions. The average was calculated over the frequency range between 0.25 and 63 Hz, where the storage modulus remained relatively stable. Since the washing test was performed at 100 rpm, corresponding to approximately 1.7 revolutions s^{-1}, the storage modulus in this frequency range may provide an approximate indication of fabric response under cyclic laundering conditions. When comparing the Young's modulus in transient conditions with the storage modulus of all the fabrics, most of them behave in a similar way in both experiments. It is especially true for fabrics containing elastane and polyamide. The 100% PET fabrics are the most affected by the application of a dynamic strain compared to the analysis in transient conditions. PET2, PET3 and PET4, which showed a low Young's modulus in the warp direction, exhibit a higher ability to store elastic energy in conditions similar to washing when it comes to deformation frequency. For PET1 and rPET, the dynamic responses were more similar than those observed under transient strain conditions, which is consistent with the broadly similar thermal transition behavior observed by DSC.

3.1.4 Thermogravimetric analysis

Thermogravimetric analysis (TGA) was conducted on all fabric samples to confirm their fiber compositions and, in the case of blended fabrics, to verify whether differences existed between warp and weft yarns. The derivative thermogravimetric curves and their deconvolutions are shown in Figure 4. Deconvolution was performed using the derivative form of a generalized logistic function, with each component assigned to a degradation step based on reference thermal degradation profiles of polyester, polyamide, and elastane fibers. Figure 4 shows a representative PET fabric, while the full set of DTG curves and deconvolutions is provided in Supplementary Figure S4.

All 100% PET fabrics exhibited two main degradation stages, corresponding to pyrolysis followed by combustion (Martín-Gullón et al., 2001). These two stages were also observed in the thermal decomposition of PAPET. Regarding polyamide, the PA fabric exhibited four different degradation stages. Previous studies have reported at least three degradation steps for polyamide under air atmosphere, with the later stages associated with char degradation after the main decomposition step (Herrera et al., 2001). All four steps were also observed in the PA-containing blended fabrics, PAEL and PAPET. Elastane has been reported to exhibit

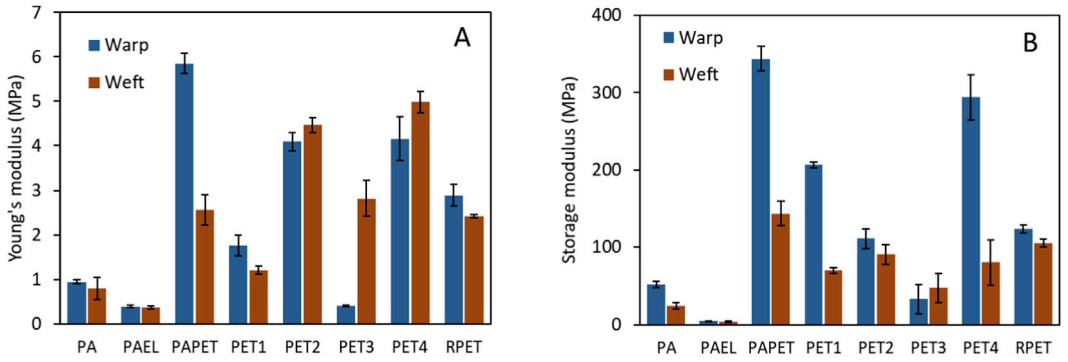

FIGURE 2
Average value of the **(A)** Young's modulus (MPa) measured in the strain rate in warp and weft direction and **(B)** the storage modulus (MPa) measured in the frequency test in warp and weft directions.

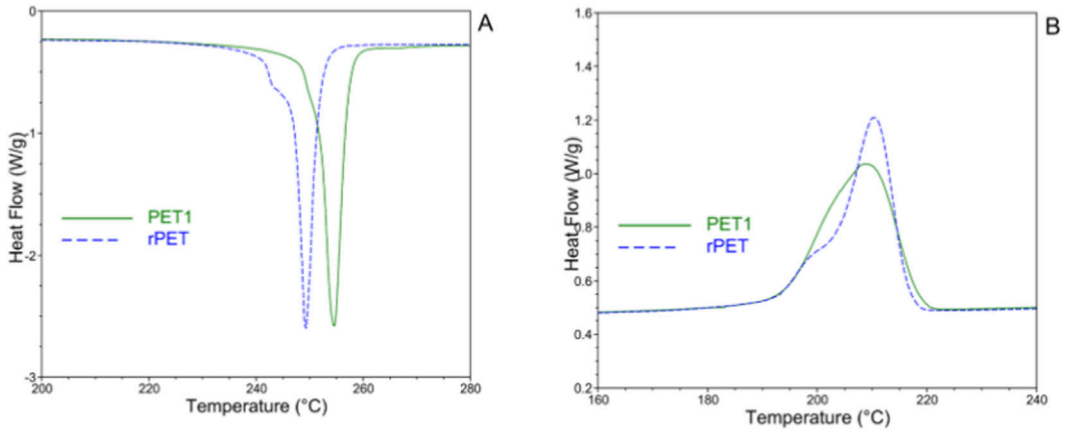

FIGURE 3
(A) Melting during heating and **(B)** crystallization during cooling transitions of rPET and PET1 in DSC analysis.

a four-step degradation process involving both oxidative and non-oxidative reactions (Boschmeier et al., 2023; Król and Pilch-Pitera, 2007). In the PAEL fabric, the final elastane-related degradation step was not clearly detected, possibly due to the relatively low elastane content in this fabric.

Deconvolution of the DTG curves allowed the mass percentage of each fiber component to be estimated in the blended fabrics. For PAEL, the estimated composition was 89.5% polyamide and 10.5% elastane, which was reasonably close to the supplier-reported composition of 86% PA and 14% EL. For PAPET, the estimated composition was 46.5% PET and 53.5% PA, in agreement with the nominal 50:50 blend ratio.

For these blended fabrics, warp and weft yarns were analyzed separately by TGA. In both PAPET and PAEL, the warp and weft yarns were found to have the same polymer composition. Therefore, the directional differences observed in DMA are more likely attributable to fabric structure, yarn arrangement, and mechanical anisotropy rather than to differences in yarn composition. Because the DTG profiles of the warp and weft yarns were same for both PAPET and PAEL, one representative plot for each fabric is provided in Supplementary Figure S4.

3.2 Microplastic fiber release: count-based and mass-based evaluation

MPF shedding was evaluated using both count-based (MPFs/g) and mass-based (mg/g) metrics to compare the magnitude and mechanisms of release among different fabrics. Because particle number and length distribution are highly relevant to environmental transport and potential exposure, count-based results were emphasized together with mass-based indicators rather than interpreted in isolation.

3.2.1 Mass-based evaluation of MPF release

Mass-based analysis quantified MPF release through changes in fabric mass loss and filter mass gain normalized per gram of fabric (mg/g) (Figures 5A,B).

Among all fabrics, PET2 exhibited the highest fabric mass loss (approximately 10.2 mg/g) and the highest filter mass gain (approximately 10.0 mg/g), likely due to its open fabric structure and lower yarn density, which may increase yarn exposure to mechanical agitation during washing. In contrast, PET3 showed low fabric mass

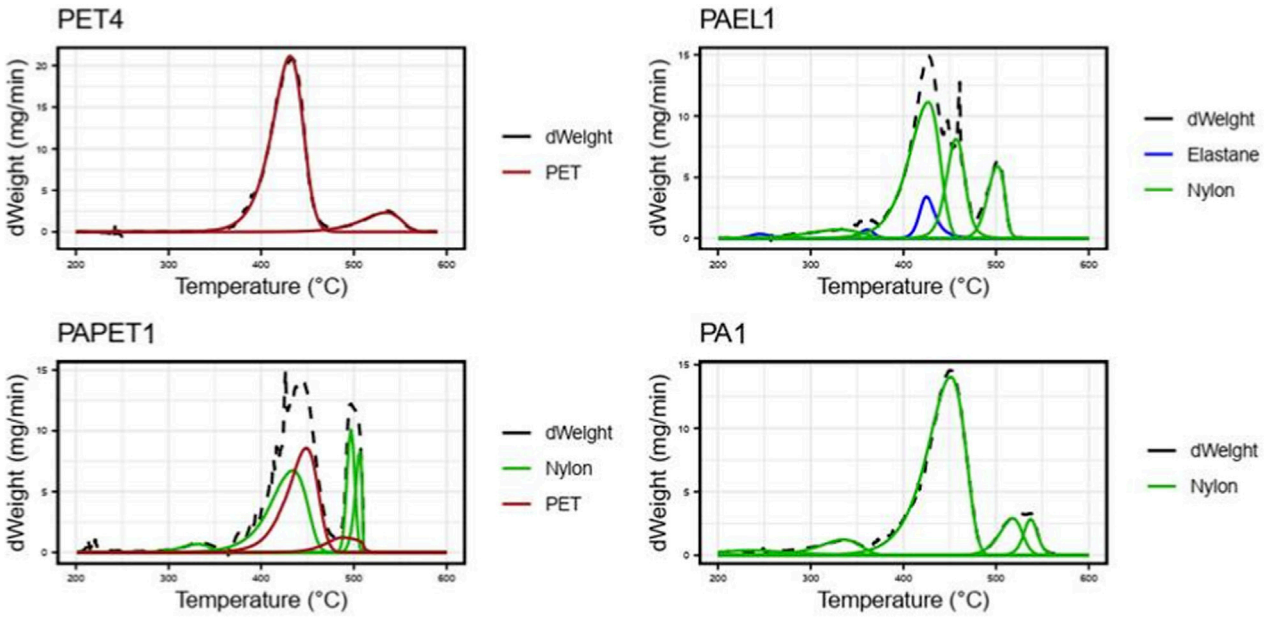

FIGURE 4
Deconvolutions of DTG curves of the fabrics, assigned by origin, whether PET, Elastane, or Nylon (polyamide).

loss (~0.4 mg/g) and low filter mass gain (~0.6 mg/g), suggesting relatively high resistance to fiber detachment under the washing conditions used. PET1 presented a notable difference between fabric mass loss (~5.0 mg/g) and filter mass gain (~1.0 mg/g), suggesting that gravimetric measurements based on fabric mass and filter mass do not necessarily capture the same fraction of released material. Similarly, PET4 displayed a fabric mass variation close to zero, slightly negative, but a measurable filter mass gain (~2.4 mg/g), highlighting the limitations of gravimetric measurements when mass changes are close to the detection limit of the balance. Such discrepancies may be influenced by small differences in moisture content, filter handling, retained residues, or incomplete transfer of detached material. Blended fabrics showed distinct behaviors. PAPET exhibited low fabric mass loss (~0.5 mg/g) but a relatively high filter mass gain (~2.7–2.8 mg/g), indicating a marked discrepancy between the two gravimetric measures. PAEL demonstrated relatively low shedding by mass (~0.6 mg/g fabric loss and ~0.4 mg/g filter gain). rPET and PA exhibited fabric mass losses of approximately 2.2 and 1.5 mg/g, respectively. However, their behaviors differed when filter mass gain was considered: rPET showed a filter mass gain of approximately 1.4 mg/g, compared with approximately 1.1 mg/g for PA. Overall, mass-based metrics revealed substantial variability among fabrics but also showed inconsistencies between fabric mass loss and filter mass gain, indicating that gravimetric methods alone may not fully capture fiber-release behavior. For this reason, mass-based results were interpreted together with MPF counts and length-distribution data.

3.2.2 Count-based evaluation of MPF release

Count-based analysis (expressed as MPFs/g) provided a more sensitive indicator of fragmentation behavior than mass-based metrics, as it reflects the number of released particles rather than total detached mass, as summarized in Table 2 and visualized in Figure 6.

PAEL released the most MPFs (~106 per cycle), suggesting that the elastane-containing structure may be more susceptible to fragmentation or filament separation under cyclic mechanical stress. PAPET exhibited the fewest (~20 MPFs), suggesting enhanced cohesion in the blended yarn. PA and rPET showed intermediate absolute counts (~36 and ~55 MPFs, respectively), while PET2 and PET3 displayed comparable counts (~38 MPFs). PET1 and PET4 produced fewer MPFs (~24 and ~29 MPFs), suggesting that yarn compactness and surface characteristics influenced fiber breakage. Absolute MPF counts and mass-normalized MPF release showed different rankings because specimen masses differed among fabrics. Therefore, absolute counts were used to describe total release per washing cycle, whereas MPFs/g were used for inter-fabric comparison.

After normalization by fabric weight (Figure 6), PET2 (31.67 MPFs/g) and rPET (30.74 MPFs/g) exhibited the highest MPF release intensities, followed by PAEL (26.01 MPFs/g) and PAPET (24.21 MPFs/g). In contrast, PET3 (9.51 MPFs/g) and PET4 (8.48 MPFs/g) showed the lowest emission levels, suggesting lower MPF release under the standardized washing conditions used in this study. PA (15.00 MPFs/g) and PET1 (13.15 MPFs/g) displayed intermediate behavior. The elevated MPF release observed in PET2 is consistent with its high mass loss and filter gain, suggesting combined bulk detachment and fragmentation mechanisms. Structurally, PET2 is characterized by lower yarn density compared to PET3 and PET4, which may reduce inter-yarn constraint and facilitate filament displacement under cyclic mechanical stress. One-way ANOVA performed on mass-normalized MPF release showed significant differences among fabric types, $F(7,16) = 10.39$, $p = 6.41 \times 10^{-5}$. Tukey's *post hoc* test indicated that PET2 released significantly more MPFs/g than PA, PET1, PET3, and

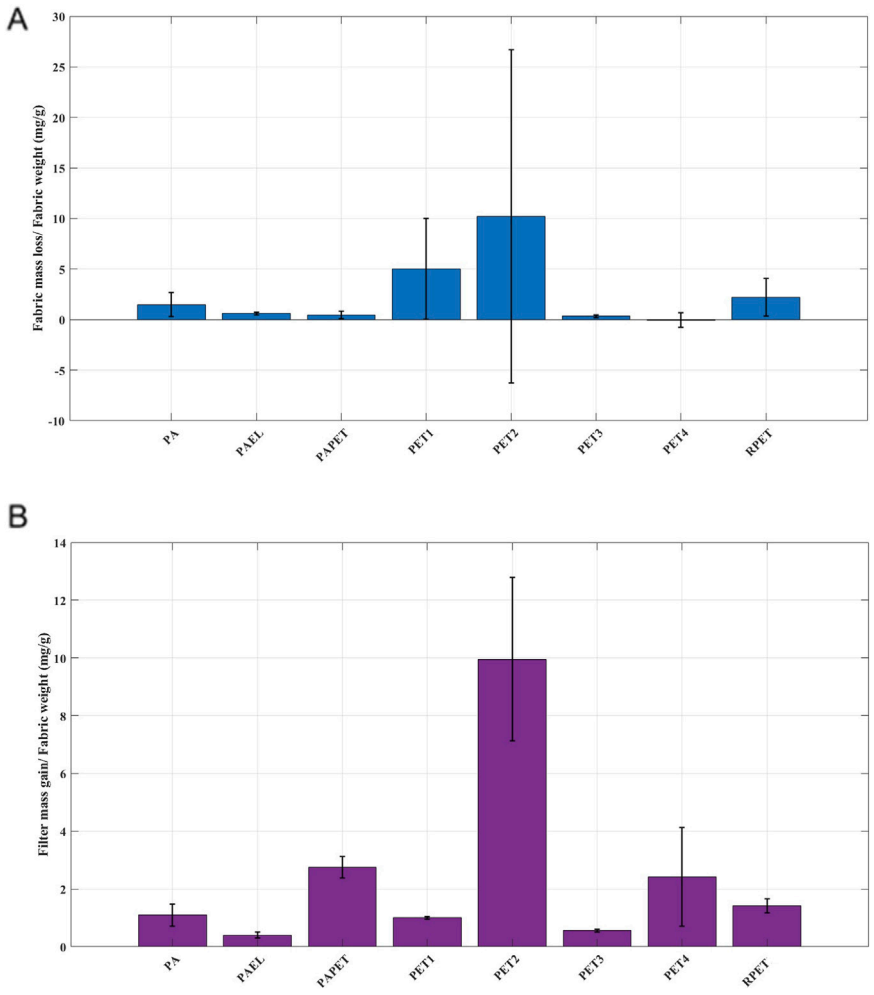

FIGURE 5
Mass-based evaluation of MPF release: **(A)** fabric mass loss normalized per gram of fabric (mg/g); **(B)** filter mass gain normalized per gram of fabric (mg/g).

TABLE 2 **Microplastic fiber count.**

Fabric	PA	PAEL	PAPET	PET1	PET2	PET3	PET4	RPET
Filter 1	34	95	25	19	34	29	33	35
Filter 2	38	105	19	28	32	29	36	55
Filter 3	36	117	17	24	48	55	17	76
Average	*36.0 ± 1.63*	*105.7 ± 8.99*	*20.3 ± 4.00*	*23.7 ± 3.68*	*38.0 ± 7.12*	*37.7 ± 12.26*	*28.7 ± 8.34*	*55.3 ± 16.74*

PET4, while rPET released significantly more MPFs/g than PET1, PET3, and PET4. PAEL also released significantly more MPFs/g than PET1, PET3, and PET4. These results support the conclusion that MPF release differed significantly among fabric types under the standardized washing conditions.

The comparison between PET1 and rPET is particularly noteworthy. Despite identical weave structures (plain weave), rPET released approximately 2.3-fold more MPFs per gram than PET1 (30.74 vs. 13.15 MPFs/g), despite exhibiting lower overall fabric mass loss. This divergence indicates that recycled polyester undergoes enhanced fragmentation rather than large-scale filament detachment. Similar trends have been reported in previous studies suggesting that thermo-mechanical recycling may induce chain scission, reduce molecular weight, and alter crystallinity, potentially increasing brittleness and fragmentation susceptibility under repeated mechanical stress. (Özkan and Gündoğdu, 2020; Akyildiz et al., 2024). However, in the present study, DSC analysis did not show marked differences in the melting or crystallization profiles of PET1 and rPET. Therefore, the higher normalized MPF release from rPET should not be attributed

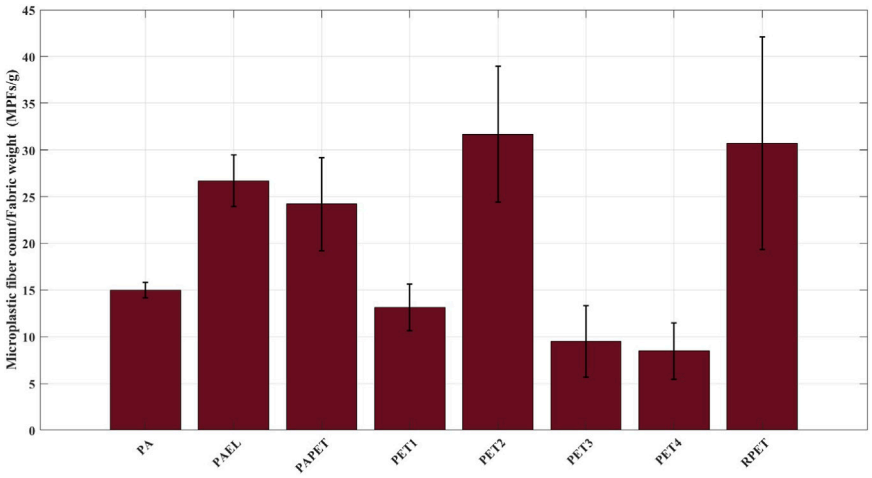

FIGURE 6
MPFs count normalized per gram of fabric (MPFs/g).

solely to crystallinity-related effects. Instead, the higher rigidity observed for rPET in DMA may have reduced its ability to dissipate cyclic mechanical stresses during washing, promoting brittle fragmentation of weakly bound or protruding filaments. This interpretation is consistent with the higher proportion of shorter MPFs released from rPET. The lower MPF release observed in PET3 (twill) and PET4 (satin) aligns with previous findings indicating that weave structure and yarn compactness influence fiber mobility and abrasion resistance during laundering (Raja Balasaraswathi and Rathinamoorthy, 2021; Cui and Xu, 2022). Blended fabrics also reveal distinct fragmentation patterns. PAEL (26.01 MPFs/g) exhibited substantially higher release than PA (15.00 MPFs/g), suggesting that elastane incorporation may increase fatigue-induced fiber separation under cyclic deformation. Conversely, PAPET displayed high MPF counts (24.21 MPFs/g) despite minimal fabric mass loss, indicating detachment of numerous lightweight fragments rather than significant bulk fiber removal. Overall, count-based results demonstrate that fabric structure and filament integrity may exert a stronger influence on MPF release than polymer chemistry alone under the tested conditions. While PET-based materials dominate global fiber production, their shedding behavior varies substantially depending on textile structure and material origin. Therefore, MPFs/g provides a more representative metric for evaluating environmental emission potential than mass-based measurements alone. Several studies have emphasized that particle number is a more representative metric of environmental exposure than total mass, particularly for small synthetic fibers that may be transported and ingested more readily (Napper and Thompson, 2016; Cai et al., 2020).

The MPFs length distribution depicted in Figure 7 reveals distinct shedding profiles for each fabric type based on four length intervals: < 0.5 mm, 0.5–1 mm, 1–2 mm, and > 2 mm. PA released MPFs predominantly within the 0.5–1 mm range (~55%), followed by 1–2 mm (~25%) and < 0.5 mm (~18%). PAEL displayed an exceptionally narrow distribution, with nearly all MPFs falling within the 0.5–1 mm range, suggesting a relatively uniform fragmentation mechanism that may be related to cyclic deformation of the elastane-containing structure. PAPET exhibited a wider distribution, releasing approximately 50% of MPFs between 0.5 and 1 mm, 25% in the 1–2 mm range, and 25% below 0.5 mm PET1 and PET2 both showed diverse distributions, with PET1 shedding more within the 0.5–2 mm range and PET2 exhibiting a evener spread across all intervals, including a noticeable proportion above 2 mm—suggesting structural weaknesses and lower compactness. PET3 and PET4, characterized by twill and satin weaves, respectively, released a majority of MPFs shorter than 0.5 mm. This suggests that, although total MPF release was low, the fibers that were released may have originated mainly from localized surface abrasion or breakage of exposed filament ends. RPET revealed a more balanced distribution, with ~40% of MPFs under 0.5 mm, ~35% between 0.5 and 1 mm, and the remainder distributed across longer ranges, possibly reflecting differences in mechanical response, filament integrity, or processing history associated with the recycled material. A direct comparison between PET1 and rPET—fabrics with identical weave structures—further emphasizes the influence of material origin on MPFs' shedding. While PET1 predominantly released mid-length (0.5–2 mm), rPET exhibited a higher proportion of shorter (<0.5 mm), suggesting greater fragmentation. This difference may be related to the stiffer mechanical response of rPET observed in DMA, which could reduce stress dissipation during cyclic washing and promote brittle fragmentation of weakly bound or protruding filaments. However, because DSC did not show marked differences in thermal transition behavior between PET1 and rPET, crystallinity-related explanations should be considered with caution.

The measured MPF length distribution is environmentally relevant because fiber size and shape can influence transport, persistence, retention, and biological interactions in downstream systems. Synthetic microfibers have been reported as a major fraction of environmental microplastics, and their interaction with aquatic organisms depends partly on particle morphology and retention behavior (Bour et al., 2020; Rebelein et al., 2021). Shorter MPFs, particularly those below 0.5 mm, may remain suspended more easily, be transported over longer distances, pass

10.3389/fmats.2026.1891868

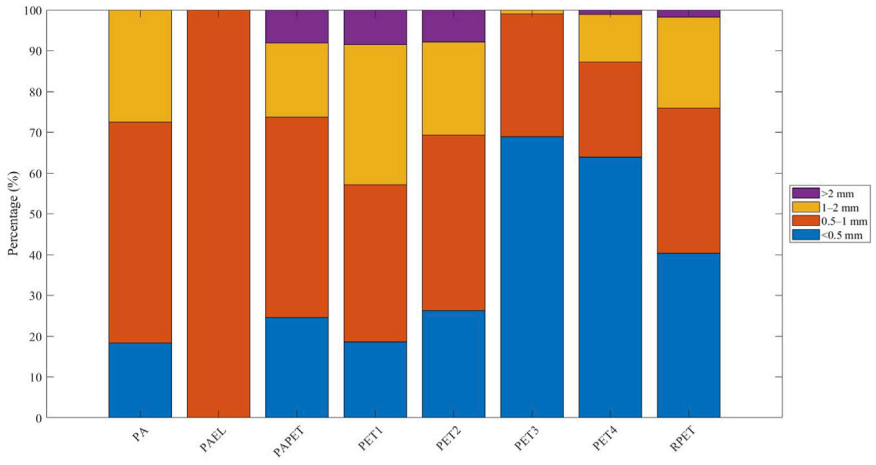

FIGURE 7
Length distribution of released microplastic fibers according to four size intervals: < 0.5 mm, 0.5–1 mm, 1–2 mm, and >2 mm.

more readily through filtration or wastewater treatment barriers, and become available for ingestion by smaller aquatic organisms (Edo et al., 2020; Nguyen et al., 2025). In contrast, longer fibers may exhibit different settling behaviors and may have a greater potential for entanglement or retention in digestive or respiratory structures. Therefore, fabrics releasing a higher proportion of short MPFs, such as rPET, PET3, and PET4 in this study, may contribute differently to downstream exposure than fabrics releasing fewer but longer fibers.

3.2.3 Comparative assessment between count- and mass-based methods

The relationship between MPFs counts and mass-based release metrics is illustrated in Figure 8, which presents MPFs released per unit of fabric mass loss (Figure 8A) and per unit of filter mass gain (Figure 8B).

These comparative graphs reveal important differences in shedding behavior across different fabric types. The number of MPFs released per unit mass of released material was calculated by dividing the MPF count by the mass of released material normalized to fabric mass, according to Equation 1:

$$Microplastic\ fiber\ count\ per\ mass = n_{MPFs}\left(\frac{m_{MPFs}}{m_{fabric}}\right)^{-1} \quad (1)$$

In Equation 1, n_{MPFs} refers to the number of MPFs counted in the filters, mfabric represents the mass of the fabric that released those MPFs, and m_{MPFs} corresponds to the difference in mass detected by weighing the filters or the fabrics before and after washing. In Figure 8A, the m_{MPFs} corresponds to the difference in mass of the fabrics, and in Figure 8B, m_{MPFs} corresponds to the difference in mass of the filters before and after filtering. Both represent the mass of the released MPFs but measured using two different methods.

In terms of MPFs per milligram of fabric mass loss (Figure 8A), PAPET and PAEL exhibited notably high MPFs counts, indicating that many MPFs per unit mass, suggesting a higher count-to-mass ratio MPFs were generated per unit of fabric loss. This suggests that for blended fabrics and elastane-containing materials, MPFs count may provide a more sensitive measure of emission potential compared to mass alone. In contrast, PET1 and PET2 displayed relatively low MPFs counts per milligram of mass loss, despite experiencing substantial overall mass loss. This indicates that these fabrics tend to release heavier and potentially thicker MPFs, which reduce the count-to-mass ratio. PET3, PET4, and rPET demonstrated intermediate behaviors, suggesting a more balanced distribution between MPFs size and weight. Notably, PET4 exhibited a particularly low MPFs count per mass loss, consistent with the idea that its satin weave structure promotes the release of fewer but heavier MPFs. PA (polyamide) showed moderate MPFs release normalized by mass loss, consistent with earlier findings on its relatively stable size distribution.

When evaluating MPFs per milligram of filter mass gain (Figure 8B), additional insights into MPFs size and capture efficiency emerged. PAEL again showed an exceptionally high MPFs count relative to filter mass, reinforcing that elastane-containing fabrics generate numerous smaller MPFs. RPet also exhibited higher counts relative to filter mass gain compared to most PET fabrics, suggesting that recycled fibers, weakened during the recycling process, release smaller and lighter MPFs more readily. Conversely, PET1, PET2, PET3, PET4, PAPET, and PA demonstrated relatively low MPF counts per unit of filter mass gain. This observation suggests that these fabrics may release fewer but heavier fibers, which could have different transport and retention behavior in aquatic environments compared with smaller fragments.

Overall, these results highlight that count-based and mass-based approaches offer complementary information. Mass loss alone may underestimate the environmental relevance of fabrics that produce numerous small MPFs, whereas count-based metrics better capture fragmentation patterns. Therefore, combining mass, count, and length-distribution data provides a more complete assessment of MPF release behavior, particularly for blended and elastane-containing textiles.

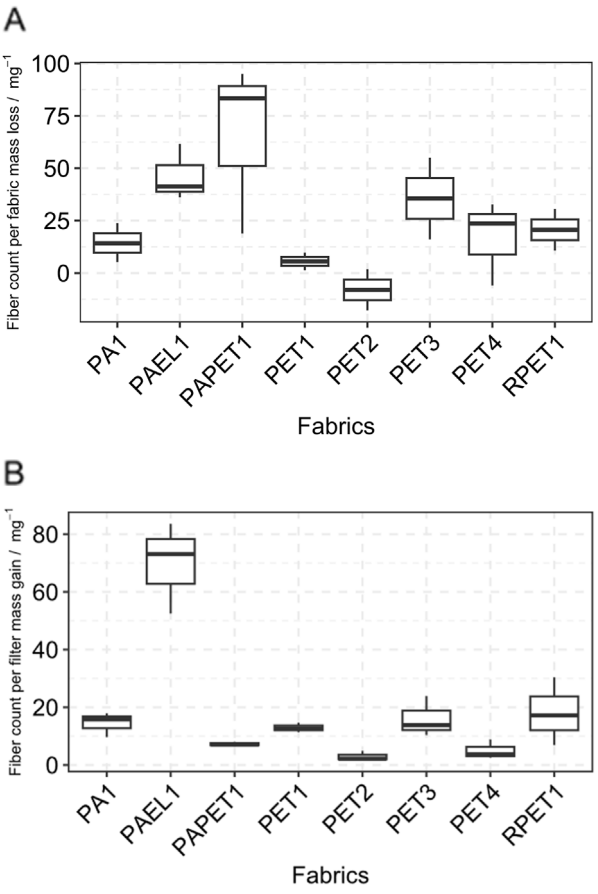

FIGURE 8
Count-to-mass comparison of MPF release: **(A)** MPFs released per unit fabric mass loss and **(B)** MPFs released per unit filter mass gain.

3.3 SEM analysis

SEM was employed to investigate the surface morphology of fabrics before and after standardized laundering, providing visual confirmation of structural changes and MPFs release mechanisms (Supplementary Figure S6). The pre-wash images show well-organized yarn arrangements and smooth fiber surfaces across all samples. Plain weaves can be seen in PA, PAEL, PAPET, PET1, PET2, and rPET, exhibiting tightly packed and uniform textures, while more open configurations were observed in samples like PET2. After laundering, notable surface degradation was observed, varying by fabric type and structure. The PA fabric exhibited fiber-end protrusion, where individual filaments were visibly displaced from the yarn bundle, indicating mechanical loosening due to agitation. In PAEL, this effect was more pronounced, with broken and unraveled filaments protruding from the surface—likely exacerbated by the elastane content, which may undergo fatigue and deformation under mechanical stress. PET3 and PET4, which feature twill and satin weaves, respectively, showed minimal surface disruption after washing. Only occasional fiber displacement or abrasion was observed, suggesting resistance to fiber detachment that may be associated with yarn compactness, smoother surface interactions, and improved stress distribution, despite their lower binding coefficients. Overall, these SEM images support the shedding patterns observed in quantitative analyses. Key post-wash degradation mechanisms, such as fiber-end protrusion, fibrillation, and filament separation, were closely associated with fabric structure, inter-fiber cohesion, and mechanical resilience. rPET and PAEL appeared more prone to producing shorter MPFs, whereas PET3 and PET4 showed improved MPF retention under the washing conditions used. However, SEM observations were qualitative and should be interpreted as supporting evidence rather than as direct quantitative confirmation of MPF release.

3.4 PCA of fabric properties and shedding behavior

PCA was conducted to explore associations among fabric characteristics, mechanical performance, structural configuration, and MPF release behavior (Figure 9). The PCA input matrix included individual replicate data from eight fabric types tested in triplicate, resulting in 24 observations. This replicate-based approach allowed both between-fabric differences and within-fabric experimental variability to be represented in multivariate analysis. Because the observations were grouped within eight fabric types, PCA was interpreted as an exploratory tool to identify associations among textile parameters and MPF release behavior rather than as a predictive or causal model. The first two components explained 65.1% of the total variance (PC1 = 39.09%, PC2 = 26.02%).

To further interpret the PCA and quantify the relative contribution of each variable, PC1 and PC2 loadings were examined. Variables with higher absolute loading values were considered the main contributors to sample separation along each principal component, and percentage contributions were calculated from squared loadings. The corresponding loading and contribution values are reported in Supplementary Table S2. PC1 appeared to represent a contrast between structural compactness and mechanical rigidity. Parameters such as basis weight, ends and picks per cm, yarn diameter, thickness, and yarn count loaded negatively, while Young's modulus, storage modulus, binding coefficient, and released MPFs per fabric weight loaded positively. The strongest contributors to PC1 were ends and picks per cm, basis weight, MPF count, yarn count, yarn diameter, and thickness, indicating that PC1 was mainly associated with fabric compactness, yarn density, dimensional structure, and release behavior.

Positive PC1 scores were associated with greater mechanical rigidity and higher normalized MPF release, whereas negative PC1 scores were associated with more compact or dimensionally substantial fabrics, including higher basis weight, greater thickness, and higher yarn density. PET2, located on the positive side of PC1, combined low basis weight (50 g/m^2) with an open plain-weave structure, resulting in poor inter-fiber cohesion and elevated shedding. rPet also occupied the positive PC1 region, consistent with its high normalized release value (30.74 MPFs/g) and its relatively stiff mechanical response. This is consistent with the hypothesis that rPET shedding in this study may be associated with reduced stress-dissipation capacity during cyclic washing rather than crystallinity differences alone.

PC2 appeared to differentiate fabrics mainly according to fiber composition and weave-related variables, binding coefficient,

10.3389/fmats.2026.1891868

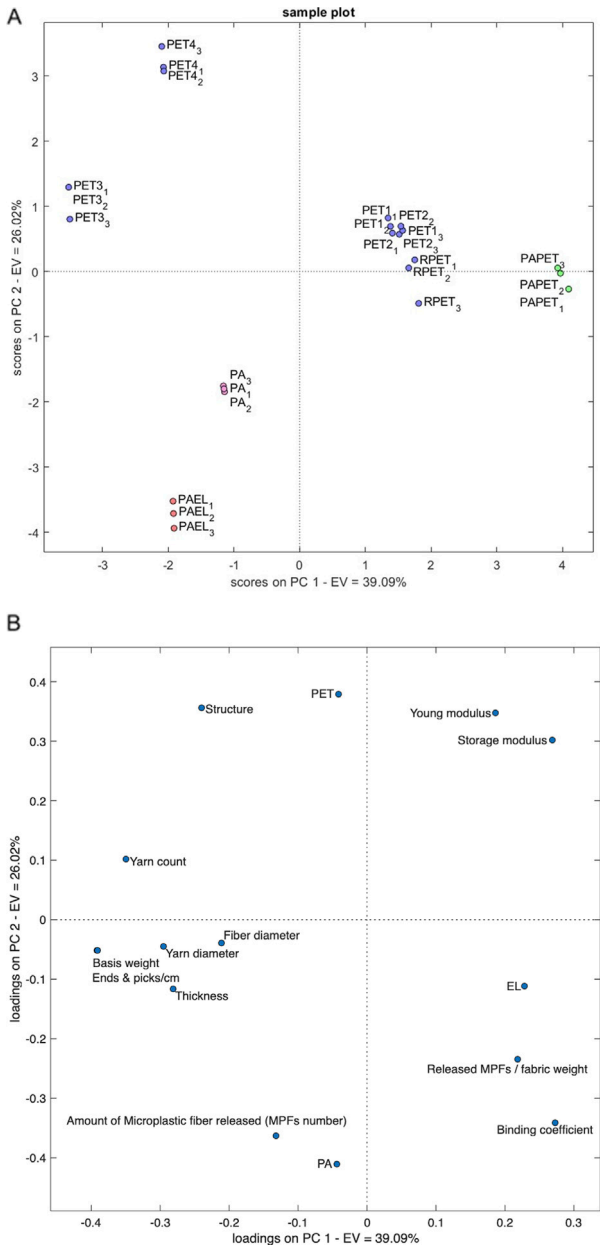

FIGURE 9
PCA of fabric properties and shedding behavior: **(A)** scores plot; **(B)** loadings plot.

and mechanical response. Positive loadings corresponded to PET-based fabrics and weave-related variables, while negative loadings were associated with PA and elastane components. The strongest contributors to PC2 were PA content, PET content, MPF count, weave structure, Young's modulus, binding coefficient, and storage modulus. Positive PC2 loadings were associated with PET content, weave structure, Young's modulus, and storage modulus, whereas negative PC2 loadings were associated with PA content, binding coefficient, MPF count, and released MPFs per fabric weight. PET3 and PET4, corresponding to twill and satin weaves, respectively, exhibited high PC2 scores, indicating that weave structure and yarn organization were important differentiating features among the low-shedding polyester fabrics. Overall, the exploratory PCA suggested that MPF release was associated with the balance between yarn cohesion, fabric compactness, binding coefficient, and mechanical response. Open structures may facilitate filament displacement, whereas localized abrasion of exposed filament ends may contribute to release even in more compact fabrics. Because PCA is an unsupervised exploratory method, these results should be interpreted as multivariate associations rather than causal contributions of individual parameters to MPF release.

Although the present study provides insight into the structural and mechanical factors associated with MPF release, several limitations should be considered. The analysis was limited to eight selected woven continuous-filament synthetic fabrics and one standardized laundering protocol; therefore, the results should not be generalized to all textile types or laundering conditions. The washing parameters were kept constant to isolate the influence of fabric structure, yarn density, filament cohesion, and mechanical response on MPF release. Washing was performed without detergent according to ISO 4484 (2023), which enabled controlled comparison among fabrics and reduced potential interference from detergent residues during gravimetric filter analysis, but may not fully reproduce real household laundering conditions. The potential effects of fabric finishing treatments, dyeing processes, spinning history, and manufacturing conditions were also not independently assessed, although these factors may influence yarn cohesion, surface morphology, and MPF shedding behavior. Finally, PCA was exploratory and should be interpreted as identifying associations rather than causal relationships.

4 Conclusion

This study demonstrates that MPF release from woven synthetic fabrics is strongly associated with fabric-level structural and mechanical properties rather than polymer composition alone. Among the tested fabrics, PET2 and rPET showed the highest normalized MPF release, indicating that open fabric structure, lower compactness, recycled fiber origin, and mechanical rigidity may increase shedding during washing. In contrast, PET3 and PET4, corresponding to twill and satin constructions, showed lower MPF release, suggesting that yarn organization, fabric compactness, and weave architecture can contribute to improved fiber retention.

The comparison between PET1 and rPET further showed that fabrics with similar weave structures may exhibit different shedding behavior depending on fiber origin and mechanical response. rPET released approximately 2.3-fold more MPFs/g than PET1 and also showed a higher proportion of shorter MPFs, which may be related to reduced stress-dissipation capacity and fragmentation of weakly bound or protruding filaments during cyclic washing. Elastane-containing PAEL also showed high MPF counts, suggesting that repeated deformation and fatigue of elastic structures may contribute to filament separation.

The exploratory PCA supported these findings by showing that MPF release was associated with a combination of yarn density, fabric compactness, binding coefficient, and mechanical

response. These results suggest that reducing textile-derived MPF release requires attention not only to fiber chemistry but also to fabric design parameters, including yarn cohesion, interlacing density, compactness, and mechanical balance. Although the study was limited to eight selected woven synthetic fabrics and one standardized detergent-free washing protocol, the findings provide useful guidance for designing synthetic textiles with lower MPF release potential.

Data availability statement

The original contributions presented in the study are included in the article/Supplementary Material, further inquiries can be directed to the corresponding authors.

Author contributions

SA: Conceptualization, Formal Analysis, Investigation, Methodology, Visualization, Writing – original draft, Writing – review and editing. MP: Conceptualization, Formal Analysis, Investigation, Methodology, Visualization, Writing – original draft, Writing – review and editing. RB: Funding acquisition, Supervision, Writing – review and editing. JL-B: Funding acquisition, Supervision, Writing – review and editing. RA: Funding acquisition, Supervision, Writing – review and editing.

Funding

The author(s) declared that financial support was received for this work and/or its publication. This study has been partially funded by Inditex Company. This study was carried out within MICS (Made in Italy–Circular and Sustainable) Extended Partnership and received funding from the European Union Next-Generation EU (PIANO NAZIONALE DI RIPRESA E RESILIENZA (PNRR) – MISSIONE 4 COMPONENTE 2, INVESTIMENTO 1.3 – D.D. 1551.11–10–2022, PE00000004). Inditex was not involved in the study design, collection, analysis, interpretation of data, the writing of this article, or the decision to submit it for publication.

Acknowledgments

The authors are thankful to the Inditex and Technical Advice companies.

Conflict of interest

The author(s) declared that this work was conducted in the absence of any commercial or financial relationships that could be construed as a potential conflict of interest.

Generative AI statement

The author(s) declared that generative AI was used in the creation of this manuscript. The authors used generative AI to improve the graphical abstract.

Any alternative text (alt text) provided alongside figures in this article has been generated by Frontiers with the support of artificial intelligence and reasonable efforts have been made to ensure accuracy, including review by the authors wherever possible. If you identify any issues, please contact us.

Publisher's note

All claims expressed in this article are solely those of the authors and do not necessarily represent those of their affiliated organizations, or those of the publisher, the editors and the reviewers. Any product that may be evaluated in this article, or claim that may be made by its manufacturer, is not guaranteed or endorsed by the publisher.

Supplementary material

The Supplementary Material for this article can be found online at: https://www.frontiersin.org/articles/10.3389/fmats.2026.1891868/full#supplementary-material

References

Akyildiz, S. H., Sezgin, H., Yalcin, B., and Yalcin-Enis, I. (2023). Optimization of the textile wastewater pretreatment process in terms of organics removal and microplastic detection. *J. Clean. Prod.* 384, 135637. doi: 10.1016/j.jclepro.2022.135637

Akyildiz, S. H., Fiore, S., Bruno, M., Sezgin, H., Yalcin-Enis, I., Yalcin, B., et al. (2024). Release of microplastic fibers from synthetic textiles during household washing. *Environ. Pollut.* 357, 124455. doi: 10.1016/j.envpol.2024.124455

Akyıldız, S. H., Sezgin, H., Yalçın Eniş, İ., Balestra, V., Marini, P., and Bellopede, R. (2025). From production to pollution: a review of microfiber release mechanisms and mitigation strategies in the textile industry. *J. Text. Inst.* 117, 1–21. doi: 10.1080/00405000.2025.2547125

Balasaraswathi, S. R., and Rathinamoorthy, R. (2022). "Synthetic textile and microplastic pollution: an analysis on environmental and health impact," in *Sustainable Approaches in Textiles and Fashion. Sustainable Textiles: Production, Processing, Manufacturing and Chemistry*. Editor S. S. Muthu (Singapore: Springer). doi: 10.1007/978-981-19-0530-8_1

Balestra, V., Trunfio, F., Akyıldız, S. H., Marini, P., and Bellopede, R. (2024). Microparticles of anthropogenic origin (microplastics and microfibers) in sandy sediments: a case study from Calabria, Italy. *Environ. Monit. Assess.* 196, 993. doi: 10.1007/s10661-024-13159-z

Boschmeier, E., Archodoulaki, V.-M., Schwaighofer, A., Lendl, B., and Bartl, A. (2023). A novel quantification tool for elastane in textiles using thermal treatment. *Polym. Test.* 118, 107920. doi: 10.1016/j.polymertesting.2022.107920

Bour, A., Hossain, S., Taylor, M., Sumner, M., and Carney Almroth, B. (2020). Synthetic microfiber and microbead exposure and retention time in model aquatic species under different exposure scenarios. *Front. Environ. Sci.* 8, 83. doi: 10.3389/fenvs.2020.00083

Cai, Y., Yang, T., Mitrano, D. M., Heuberger, M., and Nowack, B. (2020). Systematic study of microplastic fiber release from 12 different polyester textiles during washing. *Environ. Sci. and Technol.* 54 (8), 4847–4855. doi: 10.1021/acs.est.9b07395

Cesa, F. S., Turra, A., Checon, H. H., Leonardi, B., and Baruque-Ramos, J. (2020). Laundering and textile parameters influence fibers release in household washings. *Environ. Pollut.* 257, 113553. doi: 10.1016/j.envpol.2019.113553

Chakraborty, M., Shrujana, K., and Karkhanis, A. (2024). "Impacts of microfiber pollutants on the global ecosystem," in *Synthetic Fabrics and Microfiber Pollution* –

an Assessment of Their Global Impact. Editor S. Priyadarshini (Springer), 161–182. doi: 10.1007/978-3-031-51792-1_9

Cui, H., and Xu, C. (2022). Study on the relationship between textile microplastics shedding and fabric structure. *Polymers* 14 (23), 5309. doi: 10.3390/polym14235309

Das, T. K., and Jesionek, M. (2024). "Synthesis, properties, and characterization of fibrous filler," in *Fiber and Ceramic Filler-based Polymer Composites for Biomedical Engineering*. Editor J. Parameswaranpillai (Springer), 63–85. doi: 10.1007/978-981-97-3909-7_4

Das, A., Dey, S., and Das, A. P. (2024). Ecotoxicological impacts of synthetic microfiber pollutants and development of sustainable mitigation strategies. *Environ. Adv.* 10, 1000638. doi: 10.1016/j.envadv.2024.1000638

Das, T. K., Jesionek, M., Ali, M. D., Ganguly, S., and Poater, A. (2026). Advancing sustainability: circular economy strategies for fibrous polymer composites. *Clean. Mater.* 19, 100381. doi: 10.1016/j.clema.2026.100381

De Falco, F., Gullo, M. P., Gentile, G., Di Pace, E., Cocca, M., Gelabert, L., et al. (2018). Evaluation of microplastic release caused by textile washing processes of synthetic fabrics. *Environ. Pollut.* 236, 916–925. doi: 10.1016/j.envpol.2017.10.057

De Falco, F., Di Pace, E., Cocca, M., and Avella, M. (2019). The contribution of washing processes of synthetic clothes to microplastic pollution. *Sci. Rep.* 9, 6633. doi: 10.1038/s41598-019-43023-x

Dey, S., Bissoyi, A., and Koteswara Reddy, G. (2024). "Synthetic microfibers: an urban emerging pollutant demanding sustainable environmental solutions," in *Emerging Microfiber Pollutants*. Editor A. Paul (Springer), 135–157. doi: 10.1007/978-3-031-62600-5_7

Dris, R., Gasperi, J., Mirande, C., Mandin, C., Guerrouache, M., Langlois, V., et al. (2017). A first overview of textile fibers, including microplastics, in indoor and outdoor environments. *Environ. Pollut.* 221, 453–458. doi: 10.1016/j.envpol.2016.12.013

Edo, C., González-Pleiter, M., Leganés, F., Fernández-Piñas, F., and Rosal, R. (2020). Fate of microplastics in wastewater treatment plants and their environmental dispersion with effluent and sludge. *Environ. Pollut.* 259, 113837. doi: 10.1016/j.envpol.2019.113837

Frost, H., Zambrano, M., Leonas, K., Pawlak, J., and Venditti, R. (2020). Do recycled cotton or polyester fibers influence the shedding propensity of fabrics during laundering? *AATCC J. Res.* 7, 32–41. doi: 10.14504/ajr.7.S1.4

Gambino, I., Terzaghi, E., Baldini, E., Bergna, G., Palmisano, G., and Di Guardo, A. (2025). Microcontaminants and microplastics in water from the textile sector: a review and a database of physicochemical properties, use in the textile process, and ecotoxicity data for detected chemicals. *Environ. Sci. Process Impacts* 27, 297–319. doi: 10.1039/d4em00639a

Gao, M., Yang, T., Som, C., and Nowack, B. (2024). Differences in the release of microplastic fibers and fibrils from virgin and recycled polyester textiles. *Resour. Conservation Recycl.* 207, 107659. doi: 10.1016/j.resconrec.2024.107659

Ghosh, S., Sinha, J. K., Ghosh, S., Vashisth, K., Han, S., and Bhaskar, R. (2023). Microplastics as an emerging threat to the global environment and human health. *Sustainability* 15 (14), 10821. doi: 10.3390/su151410821

Gou, Z., Wu, H., Li, S., Liu, Z., and Zhang, Y. (2024). Airborne micro- and nanoplastics: emerging causes of respiratory diseases. *Part. Fibre Toxicol.* 21, 50. doi: 10.1186/s12989-024-00613-6

Han, J., McQueen, R. H., and Batcheller, J. C. (2024). From fabric to fallout: a systematic review of the impact of textile parameters on fibre fragment release. *Materials* 4 (4), 27–492. doi: 10.3390/textiles4040027

Henry, B., Laitala, K., and Klepp, I. G. (2019). Microfibres from apparel and home textiles: prospects for including microplastics in environmental sustainability assessment. *Sci. Total Environ.* 652, 483–494. doi: 10.1016/j.scitotenv.2018.10.166

Herrera, M., Matuschek, G., and Kettrup, A. (2001). Main products and kinetics of the thermal degradation of polyamides. *Chemosphere* 42 (5–7), 601–607. doi: 10.1016/s0045-6535(00)00233-2

ISO 4484-1 (2023). ISO. Available online at: https://www.iso.org/standard/82238.html (Accessed March 20, 2026).

Król, P., and Pilch-Pitera, B. (2007). Phase structure and thermal stability of crosslinked polyurethane elastomers based on well-defined prepolymers. *J. Appl. Polym. Sci.* 104 (3), 1464–1474. doi: 10.1002/app.25011

Kumar, V., Singh, S., and Bhargava, P. C. (2024). "Infiltration of microfiber in marine habitats and food chain," in *Marine Microplastics and Environmental Pollution* (Boca Raton, FL: Taylor and Francis), 203–224. doi: 10.1201/9781003529903-8

Liu, J., Yang, Y., Ding, J., Zhu, B., and Gao, W. (2019). Microfibers: a preliminary discussion on their definition and sources. *Environ. Sci. Pollut. Res.* 26, 29497–29501. doi: 10.1007/s11356-019-06265-w

Martín-Gullón, I., Esperanza, M., and Font, R. (2001). Kinetic model for the pyrolysis and combustion of poly-(ethylene terephthalate) (PET). *J. Anal. Appl. Pyrolysis* 58-59, 635–650. doi: 10.1016/S0165-2370(00)00141-8

Napper, I. E., and Thompson, R. C. (2016). Release of synthetic microplastic fibres from domestic washing machines. *Mar. Pollut. Bull.* 112 (1–2), 39–45. doi: 10.1016/j.marpolbul.2016.09.025

Nawab, A., Ahmad, M., Khan, M. T., Nafees, M., Khan, I., and Ihsanullah, I. (2024). Human exposure to microplastics: a review on exposure routes and public health impacts. *J. Hazard. Mater. Adv.* 16, 100487. Article 100487. doi: 10.1016/j.hazadv.2024.100487

Nguyen, J. K., Karthikraj, R., Habyarimana, J. B., and Kim, U.-J. (2025). A review on microplastic fibers and beads in wastewater: the current knowledge on their occurrence, analysis, treatment, and insights on human exposure impact. *Sci. Total Environ.* 968, 178818. doi: 10.1016/j.scitotenv.2025.178818

Noorimotlagh, Z., Hopke, P. K., and Mirzaee, S. A. (2024). A systematic review of airborne microplastics emissions as emerging contaminants in outdoor and indoor air environments. *Emerg. Contam.* 10 (4), 100372. Article 100372. doi: 10.1016/j.emcon.2024.100372

Nyssanbek, M., Mukhametov, A., and Azimov, A. (2022). Isolation of microfibers in the processing of polyamide fabrics. *Mater. Technol.* 56 (6), 623–627. doi: 10.17222/mit.2022.621

Özkan, İ., and Gündoğdu, S. (2020). Investigation on the microfiber release under controlled washings from the knitted fabrics produced by recycled and virgin polyester yarns. *J. Text. Inst.* 112 (2), 264–272. doi: 10.1080/00405000.2020.1741760

Paul, A., Priyadarsini, S., Karakuş, S., and Behera, J. K. (2024). "Fate and accumulation of synthetic microfibers in the environment," in *Emerging Microfiber Pollutants*. Editor A. Paul (Springer), 75–96. doi: 10.1007/978-3-031-62600-5_4

Pereira, M., López-Beceiro, J., Díaz-Díaz, A. M., Álvarez-García, A., Vázquez, L. S., and Artiaga, R. (2024). Thermogravimetry as a tool to evaluate the contribution of different fabric constituents to fibre release. *J. Therm. Analysis Calorim.* 149, 10497–10509. doi: 10.1007/s10973-024-13287-1

Periyasamy, A. P. (2023). Microfiber emissions from functionalized textiles: potential threat for human health and environmental risks. *Toxics* 11 (5), 406. doi: 10.3390/toxics11050406

Periyasamy, A. P., and Tehrani-Bagha, A. (2022). A review on microplastic emission from textile materials and its reduction techniques. *Polym. Degrad. Stab.* 199, 109901. doi: 10.1016/j.polymdegradstab.2022.109901

Priyadarshini, S., Jagatee, S., and Das, A. P. (2024). *Synthetic Fabrics and Microfiber Pollution – an Assessment of Their Global Impact*. Springer. doi: 10.1007/978-3-031-51792-1_8

Raja Balasaraswathi, S., and Rathinamoorthy, R. (2021). Effect of fabric properties on microfiber shedding from synthetic textiles. *J. Text. Inst.* 113 (5), 789–809. doi: 10.1080/00405000.2021.1906038

Rathinamoorthy, R., and Balasaraswathi, S. R. (2022). "Microfiber shedding of textile materials—Mechanism and analysis techniques," in *Microfiber Pollution and Textile Sustainability* (Springer), 25–48. doi: 10.1007/978-981-19-4185-6_2

Rebelein, A., Int-Veen, I., Kammann, U., and Scharsack, J. P. (2021). Microplastic fibers—Underestimated threat to aquatic organisms? *Sci. Total Environ.* 777, 146045. doi: 10.1016/j.scitotenv.2021.146045

Saha, S. C., and Saha, G. (2024). Effect of microplastics deposition on human lung airways: a review with computational benefits and challenges. *Heliyon* 10 (2), e24355. doi: 10.1016/j.heliyon.2024.e24355

Sharma, S., Biswas, M. C., and Nadda, A. K. (2024). *Microfiber Pollution: Environmental Challenges and Remediation Strategies*. Boca Raton, FL: CRC Press. doi: 10.1201/9781003838128

Sheikhi, M., Lupato, S., Bianco, C., Sethi, R., and Tiraferri, A. (2024). Plastic microfibers from household textile laundering: a critical review of their release and impact reduction. *Crit. Rev. Environ. Sci. Technol.* 54 (20), 1501–1525. doi: 10.1080/10643389.2024.2329513

Suaria, G., Achtypi, A., Perold, V., Lee, J. R., Pierucci, A., Bornman, T. G., et al. (2020). Microfibers in oceanic surface waters: a global characterization. *Sci. Adv.* 6 (23), eaay8493. doi: 10.1126/sciadv.aay8493

Textile Exchange (2025). Materials market report 2025. Accessed. Available online at: https://textileexchange.org/knowledge-center/reports/materials-market-report-2025/ (Accessed March 20, 2026).

Vassilenko, E., Watkins, M., Chastain, S., Mertens, J., Posacka, A. M., Patankar, S., et al. (2021). Domestic laundry and microfiber pollution: exploring fiber shedding from consumer apparel textiles. *PloS One* 16 (7), e0250346. doi: 10.1371/journal.pone.0250346

Vattanasit, U., Kongpran, J., and Ikeda, A. (2023). Airborne microplastics: a narrative review of potential effects on the human respiratory system. *Sci. Total Environ.* 904, 166745. doi: 10.1016/j.scitotenv.2023.166745